Antioxidant Chemistry: Oxidation of L-Cysteine and Its Metabolites by Chlorite and Chlorine Dioxide

James Darkwa*

Department of Chemistry, University of the Western Cape, Bellville 7535, South Africa

Rotimi Olojo, Edward Chikwana, and Reuben H. Simoyi*

Department of Chemistry, Portland State University, P.O. Box 751, Portland, Oregon 97207-0751

Received: January 17, 2004; In Final Form: April 27, 2004

The oxidation of L-cysteine and its metabolites cystine and L-cysteinesulfinic acid by chlorite and chlorine dioxide has been studied in unbuffered neutral and slightly acidic media. The stoichiometry of the oxidation of L-cysteine was deduced to be $3ClO_2^- + 2H_2NCH(COOH)CH_2SH \rightarrow 3Cl^- + 2H_2NCH(COOH)CH_2SO_3H$ with the final product as cysteic acid. The stoichiometry of the chlorite−cysteinesulfinic acid gave a ratio of 1:2, $ClO_2^- + 2H_2NCH(COOH)CH_2SO_2H \rightarrow Cl^- + 2H_2NCH(COOH)CH_2SO_3H$. There was no further oxidation past cysteic acid, and there was no evidence of sulfate formation which would have indicated the cleavage of the carbon−sulfur bond. The reaction is oligooscillatory in chlorine dioxide formation. In conditions of excess oxidant, the reaction is characterized by a short induction period followed by a rapid and autocatalytic formation of chlorine dioxide. Chlorine dioxide is formed by the reaction of intermediate HOCl with the excess chlorite: $2ClO_2^- + 2HOCl + H^+ \rightarrow 2ClO_2(aq) + Cl^- + H_2O$. Oligooscillations observed in chlorine dioxide formation result from the competition between this pure oxyhalogen reaction and reactions that consume chlorine dioxide. The rate of the reaction of chlorine dioxide with cysteine and its metabolites is fast and is of comparable magnitude with the reactions that form chlorine dioxide. The reaction of chlorine dioxide with L-cysteine is first order in both oxidant and substrate, retarded by acid, and has a lower-limit bimolecular rate constant of $405 \pm 50\ M^{-1}\ s^{-1}$, while for the reaction with L-cysteinesulfinic acid the rate constant is $210 \pm 15\ M^{-1}\ s^{-1}$. It would appear that the existence of a zwitterion on the asymmetric carbon atom precludes the formation of *N*-chloramines as has been observed with taurine and aminomethanesulfonic acid. The mechanism for the reaction is satisfactorily described by a network of 28 elementary reactions which include autocatalysis by HOCl.

Introduction

Living systems need sulfur for viability. In seawater (as well as the soil), sulfur is available as sulfate, and this sulfate is the source of sulfur for the synthesis of sulfur-containing amino acids found in proteins, e.g., cysteine and methionine.[1] Green plants use sulfate as a source of sulfur for their own biosynthesis.[2] Animals must find sulfur in a reduced organic condition in their food in order to synthesize proteins.[2] Deficiency of sulfur-containing amino acids can result in anaemia and necrosis of the liver and kidneys.[3,4] Animals cannot incorporate sulfate in proteins because they are unable to reduce it. Nearly all sulfur-type reactions in animals are oxidative, especially S-oxygenation. The major exception is the sulfide−disulfide equilibrium. All sulfur found in animal proteins comes from the S−H or S−S of the sulfur-containing amino acids.[5]

Biological thiols are products of sulfur metabolism.[6] The most important thiols in biological chemistry are cysteine, homocysteine, and glutathione. Thiols without an amino group adjacent the sulfhydryl group are easily oxidized to sulfate and a mixture of alcohols, aldehydes, and carboxylic acids (depending upon the amount and strength of oxidant). α-Aminothiols are very reactive, but will not easily cleave the C−S bond, and can thus be regenerated for further use after oxidation to the sulfenic acid or the disulfide. These thiols are strongly implicated as antioxidants in human health although the mechanistic basis for such assertions is not yet firmly established.[7] Antioxidants are needed to prevent the formation and oppose the actions of reactive oxygen species which are generated in vivo and cause damage to DNA, lipids, and proteins.[8,9] It would appear quite straightforward to attempt to mechanistically characterize the antioxidant effects of aminothiols, but so far nothing conclusive has been obtained. There are several other areas in physiological processes where thiols have been implicated. It is assumed that one of their most important roles is the forming and breaking of S−S bonds, especially in the endoplasmic reticulum (ER).[10] Protein folding in the ER often involves the formation of disulfide bonds. The oxidizing conditions required in the ER are maintained through the release of small thiols, mainly cysteine and glutathione.[11]

Our research group established a series of studies aimed at elucidating the kinetics and mechanisms of the interactions of oxyhalogen ions with small organic sulfur molecules.[12] Cysteine is one of these organosulfur molecules we have studied.[13] Cysteine is a nonessential amino acid which can be synthesized in the human body by the metabolism of methionine. By containing sulfur, cysteine can bond in a special way to maintain protein structure in the body. Cysteine is, however, only incorporated into proteins at the rate of 2.8% relative to the other amino acids, but the unique thiol side chain of this amino acid is often heavily involved in the three-dimensional stability of proteins and enzymes.[14] The side chain is also often involved in the chemistry occurring at the active sites of many enzymes.

10.1021/jp049748k CCC: $27.50 © 2004 American Chemical Society
Published on Web 05/29/2004

SCHEME 1

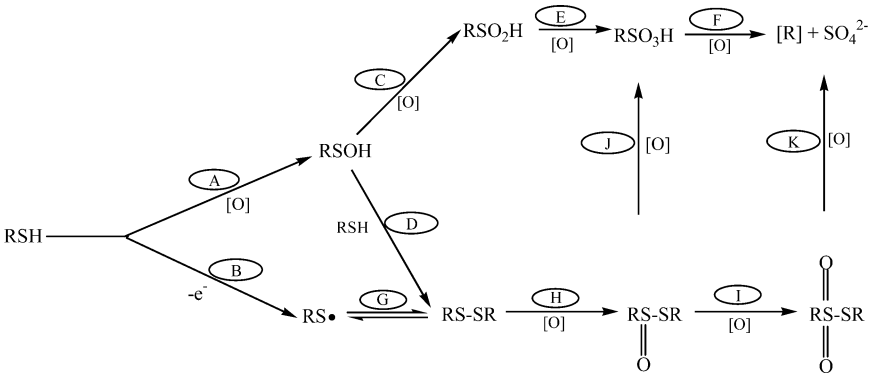

Cysteine is also critical to the metabolism of a number of essential biochemicals including coenzyme A, heparin, biotin, lipoic acid, and glutathione.[15]

Scheme 1 shows all possible reactions of a generic thiol in the human body. A number of studies have been done on process B;[16] but none to our knowledge, except one of our previous studies,[13] have been done on the S-oxygenation pathways A, C, D, E, F, and G. There is some healthy debate as to whether process B or D is the most important in the sulfide−disulfide equilibrium.[17] While, in general, sulfenic acids are rarely stable enough to be isolated,[18] sulfinic and sulfonic acids are stable enough, especially if the thiol has an amino group at the α or β carbon position.[19] We intend to report, in this article, the oxidation of L-cysteine, cystine, and L-cysteinesulfinic acid by chlorite ions. This study should enable us to evaluate the physiologically relevant reaction steps A + C + E + F; E + F and G + J (or K). This relevancy arises from the fact that physiologically, cysteine is catabolized to taurine and that in the presence of the standard P450-type enzymes, one of the major metabolites has been sulfate.[20] The major oxidizing species in chlorite oxidations is HOCl. It is known that myeloperoxidase and eosinoperoxidase catalyze the oxidation of chloride ions by H_2O_2 to produce HOCl[21] which is then deactivated by several antioxidants present in the physiological medium such as cysteine, glutathione, and taurine. The mechanism of the oxidation of these aminothiols by oxyhalogens has not yet been studied.

Experimental Section

Materials. The following analytical grade chemicals were purchased from Fisher Scientific and used without further purification: sodium chlorate, oxalic acid, sodium carbonate, perchloric acid (70%), potassium iodide, hydrochloric acid, sodium thiosulfate, starch, and sulfuric acid. L-Cysteine, cystine, L-cysteinesulfinic acid, and L-cysteic acid were purchased in analytical reagent grade quality from Sigma-Aldrich. Sodium chlorite (Sigma-Aldrich) was recrystallized from its ca. 80% technical grade purity to ∼99% assay. This was carried out from a water−ethanol−acetone mixture, and the crystals that formed were dried over a period of 1 week in a desiccator. The recrystallized chlorite was standardized iodometrically by adding acidified potassium iodide and titrating the liberated iodine against sodium thiosulfate using freshly prepared starch as indicator and employing the following stoichiometries:[22,23]

$$ClO_2^- + 4I^- + 4H^+ \rightarrow 2I_2 + Cl^- + 2H_2O$$

$$I_2 + 2S_2O_3^{-2} \rightarrow 2I^- + S_4O_6^{2-}$$

Chlorine dioxide was prepared by the standard method of oxidizing sodium chlorate in a sulfuric acid/oxalic acid mixture.[24] The stream was passed through a sodium carbonate solution before being collected in ice-cold water at 4 °C at a pH of ∼3.5.

$$2NaClO_3(s) + H_2C_2O_4\cdot 2H_2O(s) + 2H_2SO_4(aq) \rightarrow 2ClO_2(g) + 2CO_2(g) + 4H_2O + 2NaHSO_4$$

Standardization of ClO_2 was also accomplished by iodometric techniques through addition of excess acidified potassium iodide and back-titration of the liberated iodine against standard sodium thiosulfate using the following stoichiometry:

$$2ClO_2 + 10I^- + 8H^+ \rightarrow 5I_2 + 2Cl^- + 4H_2O$$

The results obtained were confirmed spectrophotometrically by using the absorptivity coefficient of ClO_2 of 1265 M^{-1} cm^{-1} at 360 nm.

Tests for Adventitious Metal Ion Catalysis. Water used for preparing reagent solutions was obtained from a Barnstead Sybron Corporation water purification unit capable of producing both distilled and deionized water (Nanopure). Not much difference was observed in the general reaction kinetics observed with distilled and deionized water. We utilized inductively coupled plasma mass spectrometry (ICPMS) to quantitatively evaluate the concentrations of a number of metal ions in the water used for our reaction medium. ICPMS analysis showed negligible concentrations of iron, copper, and silver and approximately 1.5 ppb of cadmium and 0.43 ppb of lead. The use of chelators to sequester metal ions gave kinetics and reaction dynamics indistinguishable from those run in deionized water and slightly slower kinetics than those from singly distilled water. The addition, however, of 1.0 μM Cu^{2+} ions showed a dramatic increase in rate of reaction, proving the acknowledged copper catalysis in reactions involving organosulfur compounds and also that our reaction media did not contain enough metal ions to affect the overall reaction kinetics and mechanisms.

Methods. Stoichiometric determinations were carried out by mixing various oxidant/reductant ratios in stoppered volumetric flasks and scanning them spectrophotometrically for ClO_2 activity over a period of 24 h. The products formed were characterized by ^1H NMR measurements using D_2O as solvent and internal standard (4.67 ppm). Reaction kinetics were followed on a Hi-Tech Scientific DX2 double-mixing stopped-flow spectrophotometer. Absorbance traces were obtained by following either the appearance or consumption of ClO_2 at 360 nm. All measurements were carried out at 25.0 ± 0.5 °C with ionic strength maintained at 1.0 M using $NaClO_4$. Qualitative

tests for the presence of sulfate were performed using $BaCl_2$ for sulfate precipitation in the presence of excess reductant. The stoichiometries of reactions involving chlorine dioxide were determined by pure titration of the oxidant into excess substrate with starch as indicator. Starch prepared with mercuric iodide as a preservative gave a deep blue-black color with excess chlorine dioxide.

Results

Stoichiometry. The stoichiometry of reaction between chlorite and L-cysteine was determined as

$$3ClO_2^- + 2H_2NCH(COOH)CH_2SH \rightarrow 3Cl^- + 2H_2NCH(COOH)CH_2SO_3H \quad (R1)$$

This stoichiometry was deduced as the highest chlorite/cysteine ratio that could be used without the production of chlorine dioxide after an incubation period of more than 24 h. This ratio was later reconfirmed by titrimetric techniques in which the excess oxidizing power was evaluated in excess oxidant conditions. Cysteic acid was the highest oxidation product formed in all oxidations. The same technique was utilized for the reaction of chlorite with cysteinesulfinic acid and the stoichiometry was evaluated as

$$ClO_2^- + 2H_2NCH(COOH)CH_2SO_2H \rightarrow Cl^- + 2H_2NCH(COOH)CH_2SO_3H \quad (R2)$$

No sulfate production was observed in both reactions, indicating that the C−S bond was not cleaved during the oxidation and that the sulfur center never attains the oxidative saturation state of +6. The chlorite−cystine reaction also gave cysteic acid as the final oxidation product with the stoichiometry

$$5ClO_2^- + 2(H_2NCH(COOH)CH_2S)_2 + 2H_2O \rightarrow 5Cl^- + 4H_2NCH(COOH)CH_2SO_3H \quad (R3)$$

Chlorine dioxide oxidations did not give clean and sharp stoichiometries because of the volatility of aqueous chlorine dioxide. This was especially so in reactions that involved long induction periods and in titrations performed in open containers. Chlorine dioxide oxidation kinetics were so rapid that this volatility was not significant for all our kinetics measurements. Chlorine dioxide also oxidized cysteine to as far as cysteic acid without the formation of sulfate:

$$6ClO_2(aq) + 5H_2NCH(COOH)CH_2SH + 3H_2O \rightarrow 6Cl^- + 5H_2NCH(COOH)CH_2SO_3H + 6H^+ \quad (R4)$$

The reaction of chlorine dioxide with cysteinesulfinic acid gave a stoichiometric ratio of 2:5 with the same cysteic acid product.

Product Identification. There were several possible products that could arise from the oxidation of a thiol, and we had to eliminate most of them to justify cysteic acid as the major oxidation product. The stability of cysteinesulfinic acid also suggested that it could be a possible product in the oxidation of L-cysteine. The absence of sulfate as evidenced by the lack of a precipitate with barium chloride clearly indicated that the oxidation did not proceed to cleavage of the carbon−sulfur bond. Previous experiments with other aminothiols had shown the formation of chloramines (and bromamines) by the further oxidation occurring at the amine center.[25,26] Proton NMR spectroscopy was used to conclusively identify products of the reaction. Figure 1, spectrum A is from pure L-cysteine in nearly neutral pH conditions. It shows what appears to be a triplet centered around 4.0 ppm from the asymmetric proton H_A. Close examination of this peak shows that it is a split doublet which is expected from the effect of the diastereotopic H_B and H_C protons (see Chart 1). Spectrum A also shows the complex doublet of a doublet split integrating as one proton each arising from the adjacent methylene protons H_B and H_C. In this L-isomer, H_B is the proton centered further upfield at 3.04 ppm and H_C is centered at 3.12 ppm. This splitting is expected due to the dissimilar environments protons H_B and H_C will experience due to proton H_A at the asymmetric center. Spectrum B is from the reaction mixture with excess chlorite, which should give stoichiometry R1. The spectrum shows the same types of protons as in spectrum A; but all are shifted downfield due to the formation of the more electron-withdrawing sulfonic acid group in cysteic acid. The coupling constants of protons H_B and H_C increase due to the steric hindrance brought about by the bulky sulfonic acid moiety which renders protons H_B (3.45 ppm) and H_C (3.62 ppm) more dissimilar. This increase in coupling constants now makes it clearer that the peak appearing at 4.37 ppm is a split doublet and not a triplet. Spectrum C is the product of excess chlorite with cysteinesulfinic acid. It shows the same type of spectrum as that observed in spectrum B, meaning that in both reactions the same product is obtained. A spectrum of pure cysteic acid (Fisher Scientific) was indistinguishable from that of spectrum C, indicating that it was the oxidation product in both cases. The reactions utilized to obtain spectra B and C were not buffered, and thus the products in spectra B and C were not at the same pH. The pH of the medium, due to the formation of the zwitterion on the asymmetric carbon, was extremely important in determining the position of all the protons in the spectrum. Spectrum C was taken at a lower pH than spectrum B due to the expected increase in acid strength in going from cysteinesulfinic acid to cysteic acid. This explains the small differences observed between spectra B and C. The peak observed at 4.6 ppm in spectrum C is due to an impurity that is generated during the commercial production of L-cysteinesulfinic acid.

CHART 1: Structure of Cysteine Showing the Chiral Center and the Diastereotopic Methylene Protons

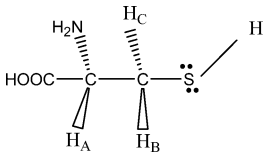

pH experiments were also performed to prove that an acidic product was formed. Figure 2 shows a pH trace of an unbuffered experimental reaction solution. This experiment shows that there is an immediate and rapid formation of acid upon addition of chlorite. The final pH of the solution could be rationalized from the stoichiometry after allowing for the acid dissociation constant of cysteic acid.

Reaction Dynamics. In stoichiometric amounts of oxidant to substrate, the reaction shows a short induction period followed by a rapid formation of chlorine dioxide which is next followed by its consumption until it is all depleted. However, in excess chlorite with ratios ($[ClO_2^-]_0/[\text{cysteine}]_0 = R$) greater than 5 and in unbuffered pH conditions, the reaction displays immediate and monotonic formation of chlorine dioxide (see trace e of Figure 3). At lower ratios chlorine dioxide concentrations reach a transient peak followed by a decrease which gives way to a

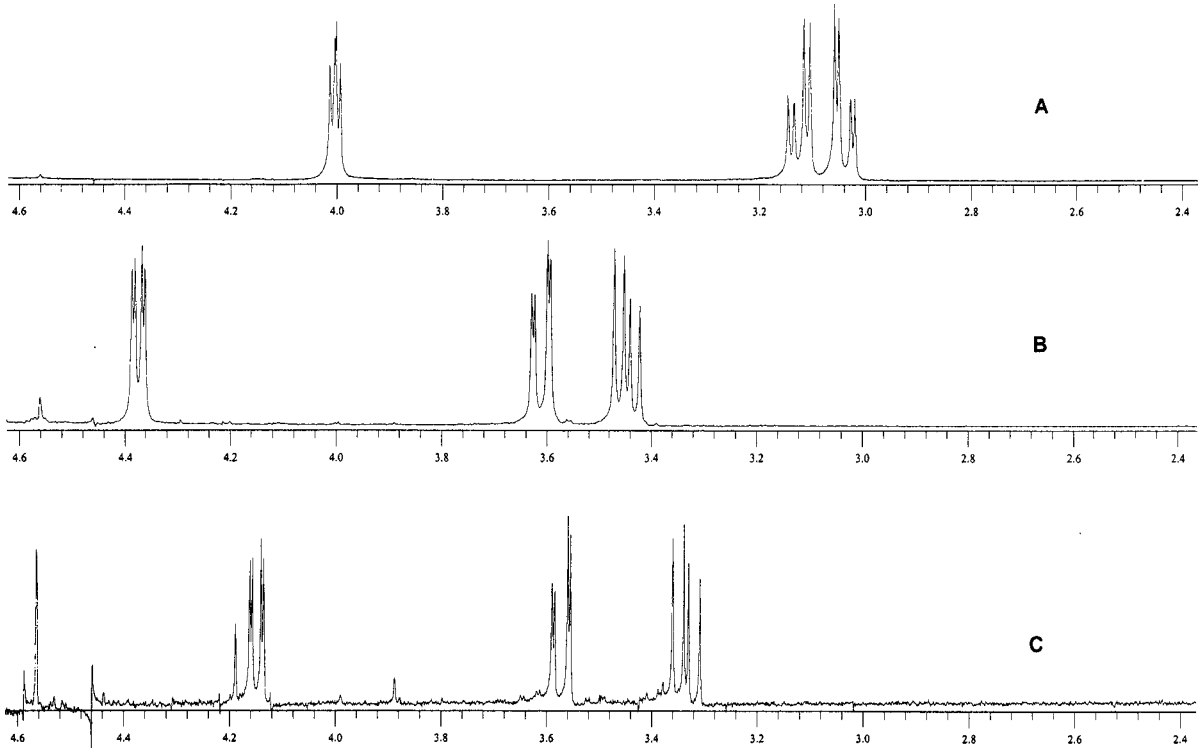

Figure 1. (A) NMR spectrum of L-cysteinesulfinic acid in nearly neutral acidic conditions. It shows the expected split doublet from protons H_B and H_C and the triplet from proton A. Each integrates as a single proton. (B) Spectrum from the products of cysteine and chlorite. Assignment: H_A (4.0 ppm); H_B (3.04 ppm); H_C 3.12 ppm). It shows basically the same spectrum as in A shifted slightly downfield due to the formation of the sulfonic acid which accompanies the oxidation of cysteine. The relative assignments with respect to field for protons H_A, H_B, and H_C in spectrum A remain unchanged. The larger coupling constants can be attributed to the larger sulfonic acid group which renders protons H_B and H_C more dissimilar. (C) NMR spectrum of the product of cysteinesulfinic acid with excess chlorite. The spurious peaks represent impurities produced in the synthesis of the cysteinesulfinic acid (Fisher Scientific). However, both spectra show that there is no change in the carbon backbone. These spectra were also indistinguishable from that of cysteic acid.

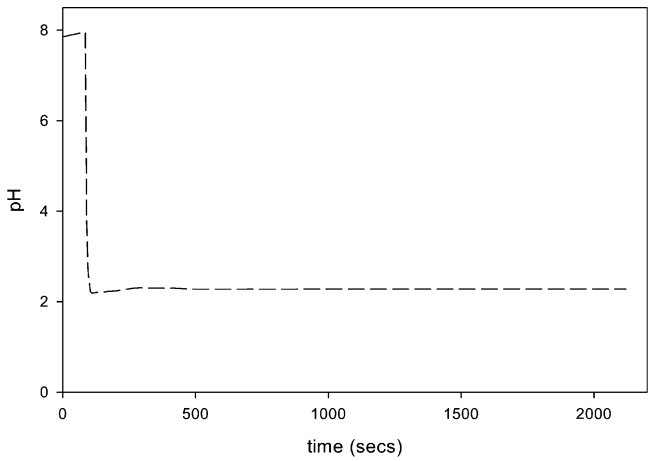

Figure 2. pH changes in the unbuffered chlorite−cysteine reaction system. This pH profile agrees with the stoichiometry which gives cysteic acid as the final product. The final pH obtained can be correlated to the expected cysteic acid formed qualified by its acid dissociation constant.

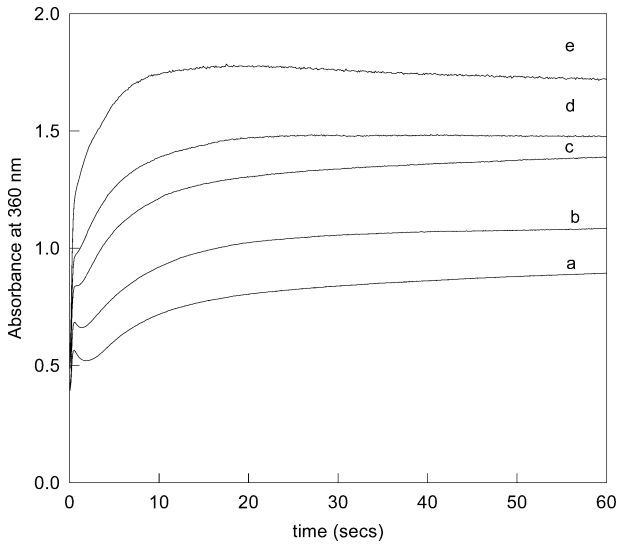

Figure 3. Variation of $[ClO_2^-]$ in cysteine oxidation by chlorite spanning chlorite/cysteine ratios of 4.0 to 7.0. High ratios show a monotonic increase in chlorine dioxide without a transient peak. $[cysteine]_0 = 5 \times 10^{-3}$ M, I = 1.0 M. $[ClO_2^-]$ = (a) 0.02 M, (b) 0.025 M, (c) 0.0275 M, (d) 0.03 M, (e) 0.035 M.

final chlorine dioxide formation which terminates at the final stoichiometric value (see traces a, b, and c in Figure 3). Figure 4 shows the effect of acid with all other initial conditions kept constant. Higher acid concentrations appear to retard the initial rapid formation of chlorine dioxide as well as its rate of consumption after the transient peak. The final chlorine dioxide concentrations in all the experiments shown in Figure 4 are the same, but the rates of attaining this final value are affected by acid. This effect of acid was a little surprising since most oxyhalogen reactions are strongly catalyzed by acid.

Although acid did not seem to enhance the initial production of chlorine dioxide, cysteine concentrations strongly catalyze the initial rapid chlorine dioxide formation (Figure 5). The data in Figure 5 show that at high cysteine concentrations the initial formation of chlorine dioxide is so rapid that it overshoots its stoichiometric value. The final stoichiometric concentration of chlorine dioxide in trace e is lower than

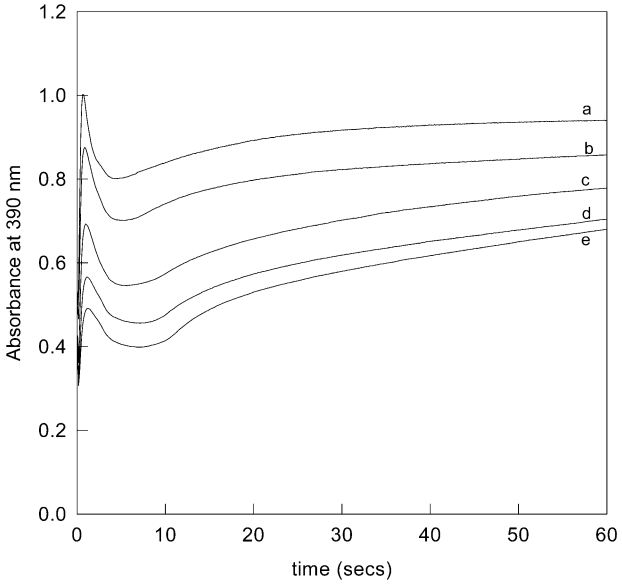

Figure 4. Variation of $[H^+]$ in cysteine oxidation by chlorite. Low acid concentrations catalyze transient formation of chlorine dioxide as well as its rapid consumption. All traces shown here gave the same final chlorine dioxide concentration. $[\text{cysteine}]_0 = 5 \times 10^{-3}$ M, $[ClO_2^-]_0 = 0.025$ M, I = 1.0 M. $[H^+]$ = (a) 0.015 M, (b) 0.045 M, (c) 0.075 M, (d) 0.105 M, (e) 0.135 M.

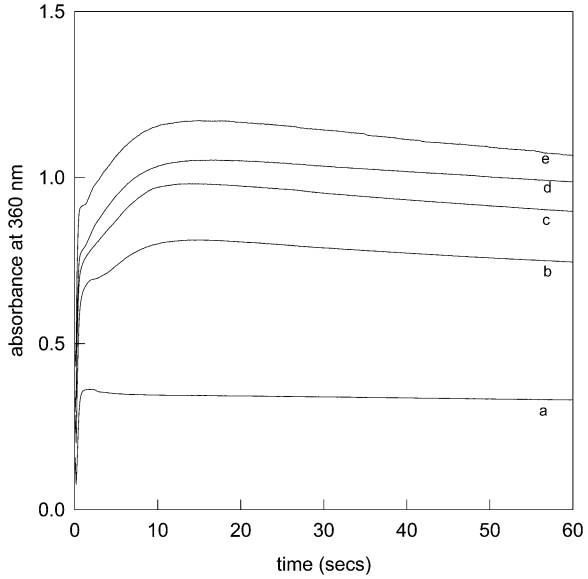

Figure 5. Variation of [cysteine] in cysteine oxidation by chlorite. At constant pH conditions, higher cysteine concentrations encourage the rapid formation of chlorine dioxide. $[ClO_2^-]_0 = 2.5 \times 10^{-2}$ M, I = 1.0 M. $[\text{cysteine}]_0$ = (a) 1.0×10^{-3} M, (b) 2.0×10^{-3} M, (c) 3.0×10^{-3} M, (d) 4.0×10^{-3} M, (e) 5.0×10^{-3} M.

that expected for trace a, and yet the accumulation of chlorine dioxide in the initial stages of the reaction in trace e ($R = 5$) far outstrips that from trace a with $R = 25$.

Oxidation of L-Cysteinesulfinic Acid. Overall, this reaction appeared to be much faster than the corresponding oxidation of cysteine and it displayed more exotic dynamics. In the absence of added acid, the reaction shows the typical sigmoidal autocatalytic formation of chlorine dioxide at low values of R (<6), (Figure 6). Surprisingly, this sigmoidal chlorine dioxide formation disappears and is replaced by a monotonic production at $R > 8$. By using an oxidant to reductant ratio above this range, e.g., $R = 10$, a series of acid dependence experiments can be performed and the pseudo-first-order rate constants (for

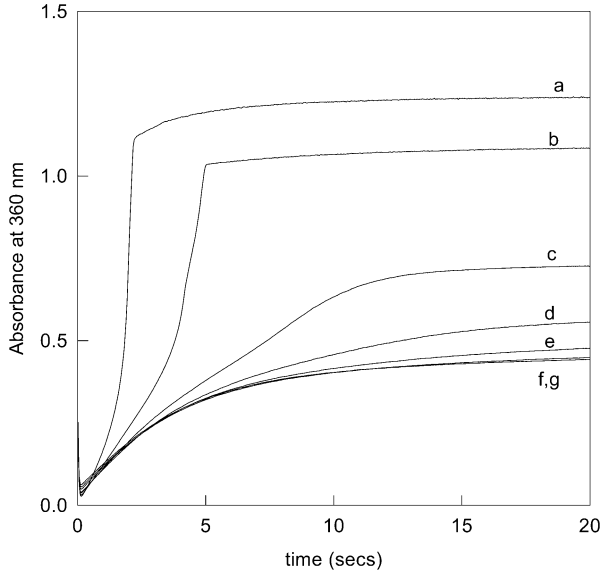

Figure 6. Variation of chlorite concentration in cysteine sulfinic acid oxidation. $[RCH_2SO_2H] = 2.5 \times 10^{-3}$ M, I = 1.0 M. $[ClO_2^-]_0$ = (a) 0.01 M, (b) 0.0125 M, (c) 0.015 M, (d) 0.0175 M, (e) 0.02 M, (f) 0.0225 M, (g) 0.025 M.

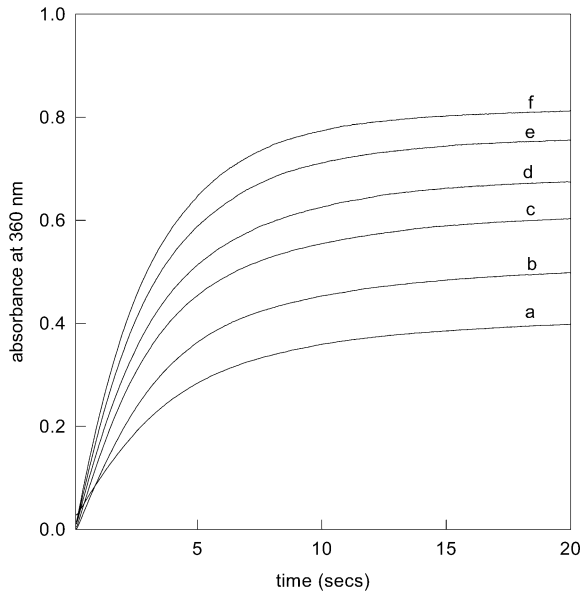

Figure 7. Acid variation in the oxidation of cysteine sulfinic acid by chlorite. Due to the high oxidant/reductant ratio, monotonic and nearly pseudo-first-order kinetics are observed in the formation of chlorine dioxide. $[ClO_2^-] = 0.025$ M, $[RCH_2SO_2H]_0 = 2.5 \times 10^{-3}$ M, I = 1.0 M. $[H^+]_0$ = (a) no acid, (b) 3.0×10^{-3} M, (c) 6.0×10^{-3} M, (d) 9.0×10^{-3} M, (e) 1.2×10^{-2} M, (f) 1.5×10^{-2} M.

the formation of chlorine dioxide) and initial rates can be evaluated and compared to initial conditions. Figure 7 shows a series of such experimental data, and they show a steady increase in rate of formation of chlorine dioxide with acid. The lower reductant concentrations are insufficient to make a significant impact on the rate of consumption of chlorine dioxide once the reaction that forms ClO_2 (referred to as reaction R6 later in this article) commences, and hence a monotonic increase in formation of chlorine dioxide will be observed.

Chlorine Dioxide Oxidation Reactions. Due to the oligo-oscillatory nature of the chlorite−cysteine reaction, it would appear that the direct oxidation of the reducing substrates in solution by chlorine dioxide may hold the key to understanding the reaction's dynamics and mechanism. Figure 8A shows that

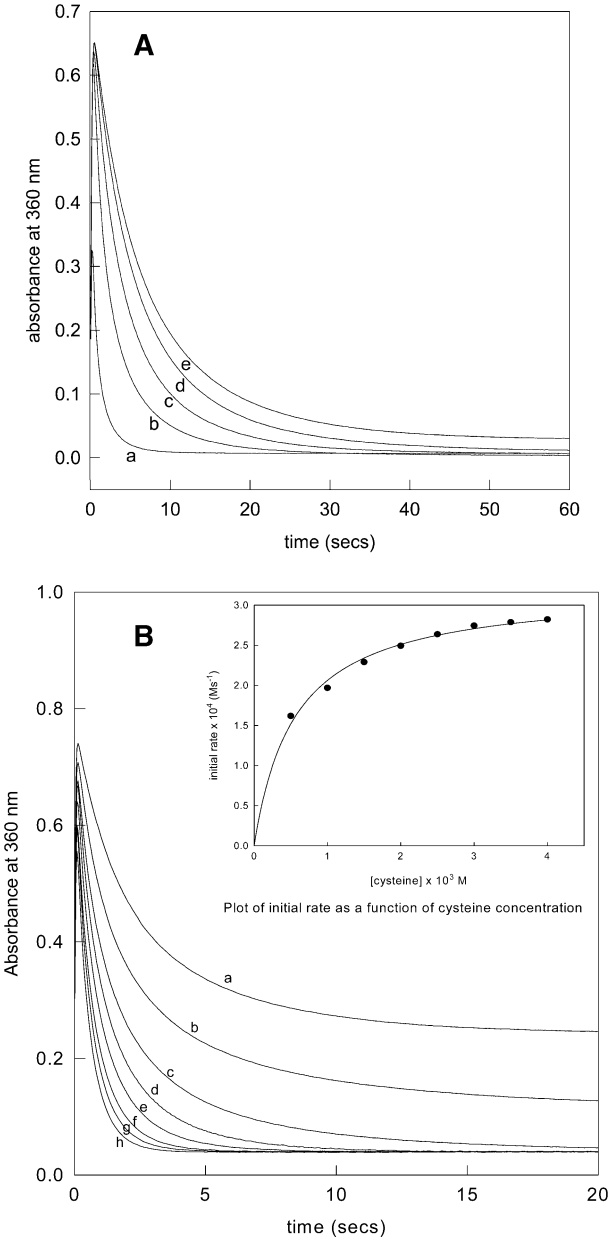

Figure 8. (A) Acid effects on cysteine oxidation by chlorine dioxide. $[\text{cysteine}]_0 = 5.0 \times 10^{-4}$ M, $[ClO_2]_0 = 7.5 \times 10^{-3}$ M, I = 1.0 M. $[H^+]_0$ = (a) no acid, (b) 1.5×10^{-3} M, (c) 6.0×10^{-3} M, (d) 1.2×10^{-2} M, (e) 1.8×10^{-2} M. (B) Variation of [cysteine] in cysteine oxidation by chlorine dioxide. $[ClO_2]_0 = 7.5 \times 10^{-4}$ M, I = 1.0 M. $[\text{cysteine}]_0$ = (a) 0.5×10^{-3} M, (b) 1.0×10^{-3} M, (c) 1.5×10^{-3} M, (d) 2.0×10^{-3} M, (e) 2.5×10^{-3} M, (f) 3.0×10^{-3} M, (g) 3.5×10^{-3} M, (h) 4.0×10^{-3} M. Inset: Plot of initial rate of reaction vs cysteine concentrations. Linearity is observed only at very low cysteine concentration with a paid saturation.

acid retards the direct oxidation of cysteine by chlorine dioxide. Figure 8B shows a positive effect on the initial rate of consumption of chlorine dioxide with cysteine, but this effect quickly saturates. Figure 9 shows the first-order dependence of the initial rate with cysteinesulfinic acid for its direct oxidation by chlorine dioxide. In this case the rates of oxidation of these two substrates appear to be of the same or comparable order. Low acid concentrations do not seem to exert any effect on the reaction of cysteinesulfinic acid with chlorine dioxide. This can be attributed to the fact that small acid concentrations will not supersede the protons being generated by the sulfinic acid itself, and so much higher acid concentrations may be needed for an effect to be observed.

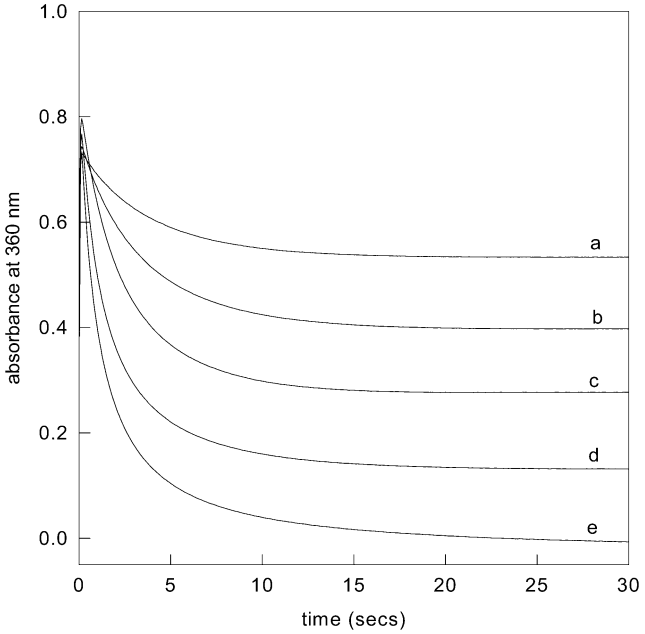

Figure 9. Variation of cysteine sulfinic acid in its oxidation by chlorine dioxide. $[ClO_2]_0 = 8.7 \times 10^{-4}$ M, I = 1.0 M. $[RCH_2SO_2H]_0$ = (a) 1.25×10^{-4} M, (b) 2.50×10^{-4} M, (c) 5.0×10^{-4} M, (d) 1.0×10^{-3} M, (e) 1.5×10^{-3} M.

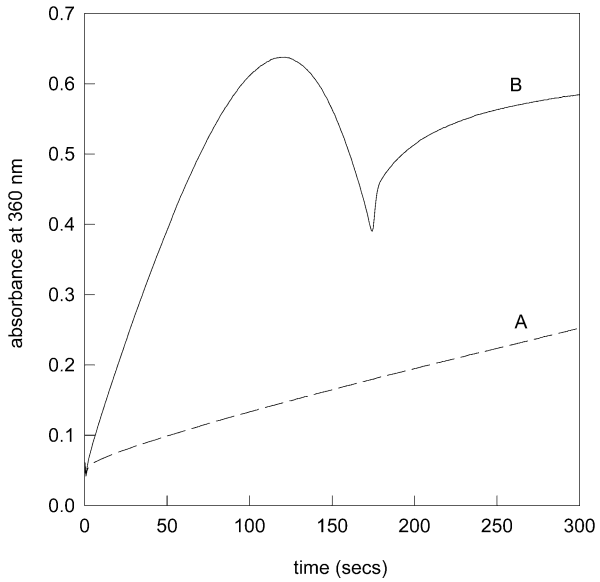

Figure 10. Absorbance traces showing cystine oxidation by chlorite in highly acidic medium; $[H^+]_0 = 0.05$ M, $[\text{cystine}]_0 = 0.01$ M (trace B). Trace A shows a control experiment without cystine. The chlorine dioxide formed in trace A is from a pure oxyhalogen reaction without the aid of a reducing substrate.

Cystine Oxidation. The most fascinating behavior was observed in the oxidation of the cysteine dimer, cystine (Figure 10) by chlorite. Cystine only dissolves in highly acidic media. As a result, the data shown in Figure 10 were obtained at lower pH conditions than those used for the rest of the data shown in this article. This particular oxidation shows a very rapid initial formation of chlorine dioxide followed by its equally rapid consumption and reformation (trace B). Trace A is a control experiment in which conditions used to obtain trace A are reproduced with the exception of cystine, which is omitted. Highly acidic chlorite solutions produce chlorine dioxide according to the stoichiometry[27]

$$5ClO_2^- + 4H^+ \rightarrow 4ClO_2(aq) + Cl^- + 2H_2O$$

Trace A represents the ClO_2 formed solely from this reaction without any contribution from the oxidation of cystine. Initial conditions used for these data ensure that all the cystine is consumed ($R = 5$). The second ClO_2 formation is the pure oxyhalogen reaction above because from about 250 s onward, the rates of formation of chlorine dioxide in both traces become approximately equal.

Mechanism

There are three major reactions occurring in the reaction mixture which are responsible for the observed oligooscillatory production of chlorine dioxide. The first reaction is the oxidation of the reductant to form products Cl^- and cysteic acid as well as the intermediate species in between: the sulfenic acid, sulfinic acid, and hypochlorous acid. The second reaction involves the rapid reaction of the hypochlorous acid with excess chlorite to produce chlorine dioxide.[28] The third reaction is the oxidation of the reducing species in the reaction mixture by chlorine dioxide. These can be summarized by the generic reaction network shown below:

$$ClO_2^- + \mathbf{Red} \rightarrow HOCl + \mathbf{Ox} \quad (R5)$$

$$2ClO_2^- + HOCl + H^+ \rightarrow 2ClO_2(aq) + Cl^- + H_2O \quad (R6)$$

$$ClO_2(aq) + \mathbf{Red} \rightarrow ClO_2^- + HOCl + Cl^- + \mathbf{Ox} \quad (R7)$$

Red represents any two-electron reducing species, e.g., cysteine; and **Ox** is the oxidized product after losing two electrons. Here reactions R5 and R7 are deliberately written unbalanced. If we assume a nonradical pathway for the reduction of ClO_2^-, then a two-electron reduction of ClO_2^- should produce HOCl as the reactive species which is involved in further oxidations of the substrates.[29] Our indicator reaction is the formation of chlorine dioxide, R6. Reaction R6 is heavily dependent on reactions R5 and R7, and thus we can make correct predictions on the rate of reaction R5 by observing R6. If reaction R6 was much faster (by an order of magnitude or two) than reactions R5 and R7, then oligooscillations will not be observed. Instead, a very sharp induction period will be observed signifying the complete consumption of the reducing substrate.[13] The effective coupling of reactions R5, R6, and R7, by virtue of being of comparable magnitudes in rate, is responsible for the exotic dynamics observed in these reaction systems. This reaction mechanism is much simpler than normal sulfur-based oxidations because the organic backbone of the thiol limits the numbers of possible intermediates that can be generated during the oxidation. The organosulfur compound, during the course of its oxidation, may be expected to produce its dimer (cystine), sulfenic acid, and its sulfinic acid. The oxyhalogen species, on the other hand, can only produce HOCl, Cl^-, $ClO_2(aq)$, and chlorate in high pH environments.[28] The oxidizing species thus are limited only to ClO_2^-, HOCl, and $ClO_2(aq)$. In low acid concentrations cystine is insoluble in water and will be expected to precipitate out during the course of the reaction if its formation is quantitative and long-lived. Since no precipitation was observed, we can exclude cystine as a major intermediate during the oxidation of cysteine in excess chlorite. Thus a full and exhaustive mechanism for the oxidation of cysteine will involve a maximum of nine reactions involving the oxidation of a sulfur center coupled to the reduction of a chlorine center (combination of three reductants and three oxidants) plus the standard oxychlorine reactions and acid−base equilibria.

Chlorite−L-Cysteine Reaction. The initial reaction step should involve a two-electron transfer from chlorite to form a sulfenic acid:

$$ClO_2^- + RCH_2SH + H^+ \rightarrow HOCl + RCH_2SOH \quad (R8)$$

R represents the asymmetric center of cysteine (HOOC)-$(H_2N)C(H)-$, and RCH_2SOH is the first metabolite, an unstable sulfenic acid. Sulfenic acids are well-known electron-deficient molecules, and they should react rapidly with the remaining thiol to give the dimeric form of cysteine, cystine ($(RCH_2S-)_2$):

$$RCH_2SH + RCH_2SOH \rightarrow (RCH_2S-)_2 + H_2O \quad (R9)$$

In the absence of further oxidant, cystine is quite stable, and it is one of the metabolites used in this study. In the presence of further oxidant, cystine should oxidize to produce two sulfenic acid molecules:

$$(RCH_2S-)_2 + 2H_2O \rightarrow 2RCH_2SOH + 2H^+ + 2e^- \quad (R10)$$

The oxidant could be any of the oxidizing species in solution: ClO_2^-, HOCl, or $ClO_2(aq)$. Sulfenic acids, due to their instability, can disproportionate into thiosulfinates,[30] but these disproportionations and dimerizations should be kinetically inconsequential in the presence of excess oxidant. Thus we would expect further oxidation to the more stable sulfinic acid:

$$RCH_2SOH + ClO_2^- + H^+ \rightarrow RCH_2SO_2H + HOCl \quad (R11)$$

The production of the sulfinic acid gives us the other metabolite whose oxidation kinetics were evaluated in this article. Our stoichiometric as well as ^1H NMR data suggest that the final oxidation product, in these conditions, would be cysteic acid:

$$RCH_2SO_2H + ClO_2^- + H^+ \rightarrow RCH_2SO_3H + HOCl \quad (R12)$$

Thus a stepwise oxidation of L-cysteine will cover the oxidation of its metabolites as well (cystine and cysteinesulfinic acid). In highly acidic conditions the oxidation of L-cysteinesulfinic acid is faster than that of L-cysteine, suggesting that the rate-determining reactions for the whole reaction scheme should lie between reactions R8 and R11. The instability of the sulfenic acid precludes reaction R11 from being rate-determining, leaving reaction R8. Reaction R8 should be able to rationalize the observed acid and species dependency of the reaction rates observed in Figures 3−5. A full explanation of these data, however, requires an understanding of the chlorine dioxide oxidation reactions which will be handled later in this article.

Chlorite−L-Cysteinesulfinic Acid Reaction. Since we have established that the oxidation of cysteine passes through cysteinesulfinic acid, the proposed mechanism for the oxidation of the sulfinic acid should then be consistent with its role in the overall oxidation of cysteine to cysteic acid. No organosulfur intermediates are possible in this simple two-electron oxidation of the sulfinic acid to the sulfonic acid. All the nonlinearities generated in this reaction system should have their genesis solely from the oxyhalogen kinetics. Figure 6 shows autocatalysis in the formation of $ClO_2(aq)$ especially at low chlorite concentrations. Acid catalysis as observed in Figure 7 would be expected if the formation of chlorine dioxide involves a pure oxyhalogen reaction. The autocatalysis observed suggests that the formation of chlorine dioxide is controlled by the reaction of an oxychlorine intermediate and not ClO_2^- as in reaction R12. HOCl

produced in R12 will react as shown in reaction R6 to form chlorine dioxide.

Chlorine Dioxide Formation. HOCl used in reaction R6 has to be autocatalytically produced for the observation of the sigmoidal kinetics in Figure 6. Another pathway for the production of chlorine dioxide would involve aqueous chlorine:

$$HOCl + Cl^- + H^+ \rightarrow Cl_2(aq) + H_2O \qquad (R13)$$

$$2ClO_2^- + Cl_2(aq) \rightarrow 2ClO_2(aq) + 2Cl^- \qquad (R14)$$

However, reaction sequence R13−R14 will only become viable if reaction R6 is slow. Reaction R6 is a composite of sequence of reaction steps that involve the often-proposed asymmetric Cl_2O_2 intermediate in aqueous environments.[29] The existence of this intermediate was proved through isotopic labeling experiments of Taube and Dodgen[31]

$$ClO_2^- + HOCl + H^+ \rightarrow Cl_2O_2 + H_2O \qquad (R15)$$

$$Cl_2O_2 + ClO_2^- \rightarrow 2HOCl + Cl^- \qquad (R16)$$

This sequence shows that one HOCl molecule will produce two HOCl molecules, and if HOCl is the major oxidant, then an autocatalytic production of chlorine dioxide from reaction R6 can be observed. We can generalize reaction R16 to apply to any two-electron reductant:

$$Cl_2O_2 + 2e^- + 2H^+ \rightarrow 2HOCl \qquad (R17)$$

This autocatalysis will not only affect chlorine dioxide formation but the oxidation of the substrate as well as its metabolites.

Consumption of Chlorine Dioxide. Parts A and B of Figure 8 show that there is a feasible and rapid reaction between cysteine and chlorine dioxide. Figure 9 shows an equally rapid reaction of the sulfinic acid with chlorine dioxide. Although Figure 8A shows that the reaction of cysteine and chlorine dioxide is retarded by acid, the reaction of the cysteinesulfinic acid with chlorine dioxide was insensitive to acid for a wide range of low acid concentrations. Chlorine dioxide is a radical species and should react very rapidly with the nucleophilic center of the thiol:

$$ClO_2(aq) + RCH_2SH \rightleftharpoons ClO_2^- + H^+ + RCH_2S^\bullet \qquad (R18)$$

$$ClO_2(aq) + RCH_2S^\bullet + H_2O \rightarrow ClO_2^- + RCH_2SOH + H^+ \qquad (R19)$$

Reactions R18 and R19 can be combined to the following composite termolecular reaction:

$$2ClO_2(aq) + RCH_2SH + H_2O \rightarrow 2ClO_2^- + 2H^+ + RCH_2SOH \qquad (R20)$$

Our kinetics data suggests that the reaction is first order in both cysteine and chlorine dioxide, which would implicate reaction R18 as rate-determining. The inhibitory effect of acid renders reaction R18 irreversible since acid would accelerate the reaction by forming the weak acid $HClO_2$ thus pushing the "equilibrium" to the right and accelerating the reaction. The inhibition should arise from the deactivation of the thiol group by protonation:

$$RCH_2SH + H^+ \rightleftharpoons [RCH_2SH_2]^+; \quad K_b \qquad (R21)$$

Thiyl radicals were not detected in our reaction system, and if produced, they should be short-lived and can only be observed with a specialized trap.[32] A kinetically indistinguishable and very plausible pathway to R18 + R19 would involve the formation of a loose adduct of the thiol and chlorine dioxide. This adduct would then react with another molecule of aqueous chlorine dioxide to release the sulfenic acid and two chlorous acid molecules:

$$ClO_2(aq) + RCH_2SH \rightleftharpoons [RCH_2S{-}ClO_2^-][H^+] \qquad (R22)$$

$$[RCH_2S{-}ClO_2^-] + ClO_2(aq) + H_2O \rightarrow RCH_2SOH + 2ClO_2^- + H^+ \qquad (R23)$$

If one assumes that the protonated thiol is inert, then the rate of reaction R20 will be given by

$$\frac{-d[ClO_2]}{dt} = \frac{k_0[RCH_2SH]_0[ClO_2(aq)]}{1 + K_b[H^+]} \qquad (1)$$

where $[RCH_2SH]_0$ is the initial concentration of cysteine used. Equation 1 can explain the observed acid retardation, and using this equation we deduced an upper-limit value of $k_{R20} = 405 \pm 50\ M^{-1}\ s^{-1}$. Further reaction would then involve the oxidation of cysteine and its metabolites by chlorite and hypochlorous acid. Sulfinic acids are not as nucleophilic as thiols, and this can explain why no appreciable effect of acid on the oxidation of L-cysteinesulfinic acid by chlorine dioxide was observed.

Overall Mechanism. We can define a complete mechanism that can adequately explain all the reactions reported in this article. A single mechanism should be able to describe the observed dynamics of the chlorite−cysteine, chlorite−cysteinesulfinic acid, chlorite−cystine, chlorine dioxide−cysteine, and chlorine dioxide−cysteinesulfinic acid reactions. This mechanism is shown in Table 1. It is comprised of three rapid protolytic equilibria (reactions M1−M3), two pure oxyhalogen reactions (M20 and M21), and two sulfur−sulfur disproportionation reactions (M27−M28). The rest of the reactions involve the oxidation of a sulfur center coupled with the reduction of a chlorine center. The complex acid dependence observed in the reaction system (see Figure 4) can be explained by the opposing effects of reactions M1, M3, M4, and M5. High acid concentrations lower the nucleophilic nature of the thiol group (reaction R21) but also protonate chlorite to form chlorous acid which is a better electrophile. Since the pK_a of chlorous acid is approximately 2.0,[33] reactions run in pH conditions lower than 2.0 should see a dominance of reaction M5 over M4 and hence acid retardation. The slower tandem of M4 + M5 in high acid stunts the production of the reactive and autocatalytic species HOCl, and hence lower chlorine dioxide concentrations are formed as seen in Figure 4. If the rates of reactions M4 and M5 are not equal, then the whole reaction system will display a strong acid effect especially in conditions where the pH of the solution is greater than or equal to the pK_a of chlorous acid. The rate law that is derived from this mechanism for the reaction of chlorite and cysteine is

$$\text{Rate} = \frac{[RCH_2SH]_0[Cl(III)]_T}{(1 + K_a^{-1}[H^+])(1 + K_b[H^+])}\{k_{M4} + k_{M5}K_a^{-1}[H^+]\} \qquad (2)$$

with a complex dependency on acid as experimentally observed.

TABLE 1: Full Mechanism[a]

no.	reaction
M1	$ClO_2^- + H^+ \rightleftharpoons HClO_2$; K_a^{-1}
M2	$OCl^- + H^+ \rightleftharpoons HOCl$
M3	$RCH_2SH + H^+ \rightleftharpoons [RCH_2SH_2]^+$; K_b
M4	$RCH_2SH + ClO_2^- \rightarrow RCH_2SOH + OCl^-$
M5	$RCH_2SH + HClO_2 \rightarrow RCH_2SOH + HOCl$
M6	$(RCH_2S-)_2 + ClO_2^- + H_2O \rightarrow 2RCH_2SOH + OCl^-$
M7	$RCH_2SOH + ClO_2^- \rightarrow RCH_2SO_2H + OCl^-$
M8	$RCH_2SO_2H + ClO_2^- \rightarrow RCH_2SO_3H + OCl^-$
M9	$RCH_2SH + HOCl \rightarrow RCH_2SOH + H^+ + Cl^-$
M10	$RCH_2SOH + HOCl \rightarrow RCH_2SO_2H + H^+ + Cl^-$
M11	$RCH_2SO_2H + HOCl \rightarrow RCH_2SO_3H + H^+ + Cl^-$
M12	$(RCH_2S-)_2 + ClO_2(aq) + H_2O \rightleftharpoons (RCH_2S)_2{\cdot}ClO_2$
M13	$(RCH_2S)_2{\cdot}ClO_2 + ClO_2(aq) + H_2O \rightarrow 2\,RCH_2SOH + HClO_2$
M14	$RCH_2SH + ClO_2(aq) \rightleftharpoons [RCH_2SClO_2]^-{\cdot}H^+$
M15	$RCH_2SClO_2^- + ClO_2(aq) + H_2O \rightarrow RCH_2SOH + 2ClO_2^- + H^+$
M16	$RCH_2SOH + ClO_2(aq) \rightleftharpoons [RCH_2S(O)ClO_2]^-{\cdot}\,H^+$
M17	$RCH_2S(O)ClO_2^- + ClO_2(aq) + H_2O \rightarrow RCH_2SO_2H + 2ClO_2^- + H^+$
M18	$RCH_2SO_2H + ClO_2(aq) \rightleftharpoons [RCH_2S(O_2)ClO_2]^-{\cdot}\,H^+$
M19	$RCH_2S(O_2)ClO_2^- + ClO_2(aq) + H_2O \rightarrow RCH_2SO_3H + 2ClO_2^- + H^+$
M20	$ClO_2^- + HOCl + H^+ \rightleftharpoons Cl_2O_2 + H_2O$
M21	$Cl_2O_2 + ClO_2^- \rightleftharpoons 2\,ClO_2(aq) + Cl^-$
M22	$RCH_2SH + Cl_2O_2 + H_2O \rightarrow RCH_2SOH + 2HOCl$
M23	$RCH_2SOH + Cl_2O_2 + H_2O \rightarrow RCH_2SO_2H + 2HOCl$
M24	$RCH_2SO_2H + Cl_2O_2 + H_2O \rightarrow RCH_2SO_3H + 2HOCl$
M25	$RCH_2SOH + HClO_2 \rightarrow RCH_2SO_2H + HOCl$
M26	$RCH_2SO_2H + HClO_2 \rightarrow RCH_2SO_3H + HOCl$
M27	$2RCH_2SOH \rightleftharpoons RCH_2SO_2H + RCH_2SH$
M28	$RCH_2SOH + RCH_2SO_3H \rightleftharpoons 2\,RCH_2SO_2H$

[a] Legend: RCH_2SH, cysteine ("R" represents the asymmetric center on cysteine); $(RCH_2S-)_2$, cystine; RCH_2SOH, cysteinesulfenic acid; RCH_2SO_2H, cysteinesulfinic acid; RCH_2SO_3H, cysteic acid.

In eq 2, $[Cl(III)]_T$ represents the total chlorine(III) species and is given by the relation

$$[Cl(III)]_T = [HClO_2] + [ClO_2^-] \quad (3)$$

In the limit of low acid concentrations, e.g., $8 > pH > 3.0$, the terms in the denominator as well as the last term drop out giving

$$\text{Rate} = k_{M4}[RCH_2SH]_0[Cl(III)]_T \quad (4)$$

In highly basic pH conditions, higher than physiological pH, the thiolate anion asserts itself, giving a different mechanism and also possibly different oxychlorine products. This range was not studied in this report.

The autocatalytic production of chlorine dioxide is fueled by the composite reaction M20 + M21 coupled with reactions M22−M24 that contain autocatalytic production of HOCl. The mechanism in Table 1 acknowledges three main oxidizing species in the reaction mixture: ClO_2^-, HOCl, and $ClO_2(aq)$. The intermediate we propose, Cl_2O_2, is only introduced to justify the observed autocatalysis. For the autocatalysis to prevail, the reactions of this intermediate, M22−M24, should be slower than the reactions involving HOCl, M9−M11. The initial oxidation of cystine should give two sulfenic acid molecules (reaction M6) which can disproportionate to thiosulfinates in the absence of excess oxidant.[30] Further oxidation of the sulfenic acid will give the sulfinic acid and finally cysteic acid. Our experimental data gave a lower-limit rate constant for direct reaction of L-cysteinesulfinic acid and chlorine dioxide of $k_{M18} = 210 \pm 15\ M^{-1}\ s^{-1}$.

This mechanism is effectively a combination of the four oxidants in the reaction mixture, $HClO_2$, ClO_2^-, HOCl, and $ClO_2(aq)$ with the four reductants, RCH_2SH, $(RCH_2S-)_2$, RCH_2SOH, and RCH_2SO_2H. Apart from the protolytic equilibria and adduct formations (e.g., reactions M12, M14, M16, and M18), all reactions involving the oxidation of a sulfur center were assumed irreversible. The sulfur−sulfur reactions, M27 and M28, are important for stoichiometric consistency in the presence of excess reductant. Under such conditions, the organosulfur species would disproportionate such that the more stable sulfinic and sulfonic acids are the dominant products. The possibility also exists for the formation of various thiosulfinates in excess reductant conditions.

Computer Simulations. We utilized a unique approach to modeling the dynamics of the oxidation of cysteine by chlorite. We modeled the simplest system first, the reaction with the smallest number of intermediates: the cysteinesulfinic acid−chlorine dioxide system. The kinetics parameters derived from this calculation were used to model the cysteine−chlorine dioxide reaction. The full reaction scheme, chlorite−cysteine, was then finally modeled using the data derived from the other two calculations. This approach was possible because we had established that the oxidation of cysteine passed through the sulfinic acid before proceeding to cysteic acid.

Cysteinesulfinic Acid−Chlorine Dioxide. Table 2 shows the very short and abbreviated mechanism used to simulate the oxidation of the sulfinic acid by chlorine dioxide. Since our experimental data have shown no strong acid dependence for this specific reaction, we could eliminate reactions M1 and M3 from the mechanism. Autocatalysis was not observed in the consumption of chlorine dioxide, and thus we did not have to include the autocatalytic production of HOCl. Reaction P1 was assumed to be bimolecular, as deduced from our kinetics data, even though it is written as termolecular. The only kinetics parameters that had to be guessed were those for P2 and P3. Kinetics parameters for P1 were estimated from this study, and those for P4 were derived from the literature.[34] The model was insensitive to values of k_{P2} and k_{P3} as long as they were not rate-determining. Figure 11A shows the reasonably good fit obtained using this very simple mechanism.

Cysteine−Chlorine Dioxide. The modeling of this system was merely an extension of that for the oxidation of the sulfinic acid. We could now utilize the kinetics parameters deduced from the model in Table 2. The mechanism used to simulate the cysteine−chlorine dioxide reaction is shown in Table 3. The observation of acid dependence in Figure 8A meant that we had to include equilibria Q14 and Q15. Since acid inhibition was observed below pH 2, we assumed that equilibrium Q15 was more important. This proved to be the case in our simulations. In this model the protonated thiol was assumed to

TABLE 2: Cysteinesulfinic Acid−Chlorine Dioxide Mechanism

no.	reaction	k_f; k_r
P1	$2ClO_2(aq) + RCH_2SO_2H + H_2O \rightarrow 2HClO_2 + RCH_2SO_3H$	210
P2	$HClO_2 + RCH_2SO_2H \rightarrow RCH_2SO_3H + HOCl$	350
P3	$RCH_2SO_2H + HOCl \rightarrow RCH_2SO_3H + H^+ + Cl^-$	5×10^3
P4	$2HClO_2 + HOCl \rightleftharpoons 2ClO_2(aq) + H^+ + Cl^- + H_2O$	1.01×10^6; 1×10^2

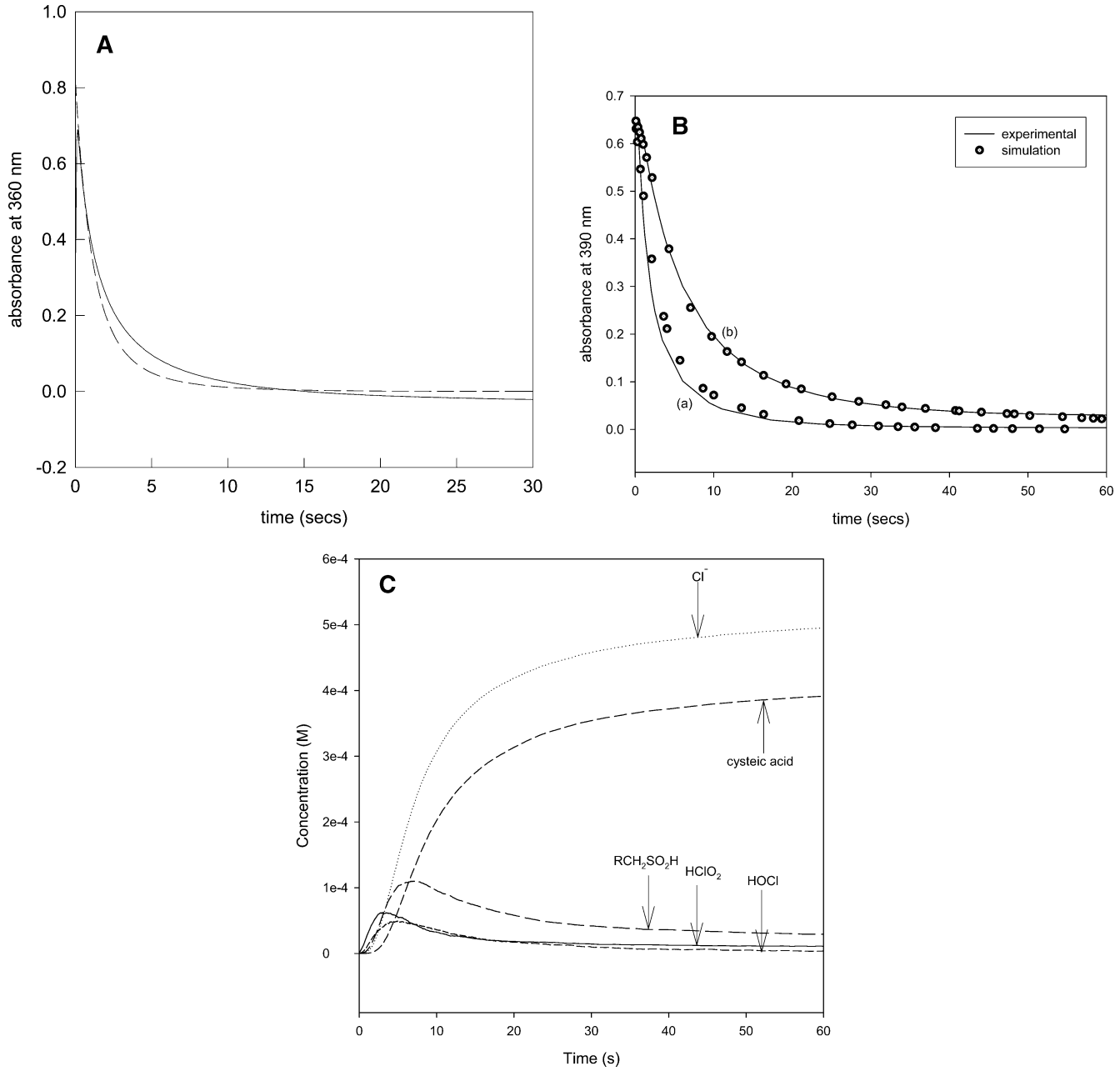

Figure 11. (A) Computer simulations using the model shown in Table 2 for the reaction between chlorine dioxide and cysteinesulfinic acid. Experimental data is represented by the solid line, while the simulations appeared as the dashed line. Conditions simulated: $[ClO_2]_0 = 8.7 \times 10^{-4}$ M; $[RCH_2SO_2H]_0 = 5.0 \times 10^{-4}$ M. (B) Modeling the chlorite−cysteinesulfinic acid reaction at two separate acid concentrations. The data simulated is shown in Figure 8A. (a) 0.0015 M H^+ and (b) 0.018 M H^+. The model shown in Table 3 correctly predicted the experimentally observed acid dependence. Solid lines represent experimental data, and symbols denote data generated from the model. (C) Extension of the model shown in trace a of part B showing the concentration trajectories for some of the products and reactive species which we could not experimentally measure. The model shows that cysteic acid is formed quantitatively after a short induction period while the sulfenic and sulfinic acids attain transient peaks before decaying to form products.

be completely inert (see eq 1). Depending upon pH, reactions Q10−Q12 could be ignored or shut down without any loss of accuracy in our model. The most important parameter in this model was k_{Q1}. Reactions Q8 and Q9 could not assert themselves at the beginning of the reaction because the concentrations of these reactive sulfur species would be vanishingly small. This reaction did not display any strong autocatalysis, and so we could eliminate (or minimize) the sequence of reactions that incorporate HOCl autocatalysis. Kinetics parameters for reaction Q1 were obtained from this study (405 $\pm$ 50 M^{-1} s^{-1}) as well as parameters for reaction Q8. The rest, apart from Q13−Q16, were estimated for best fit. At low pH conditions, the model was still accurate from the use of only reactions Q1−Q7 and Q15. Figure 11B shows the simulations fit to the data. This simple model was able to predict the observed acid dependence as well as the rate law in the form of eq 1. Using this mechanism we could also model the concentration profiles of some of the intermediates we could not measure experimentally such as the sulfinic and sulfenic acids (Figure 11C). Figure 11C shows that concentrations of the sulfenic and sulfinic acid intermediates go through transient maxima before decaying and making way for cysteic acid. Cysteic acid shows a short induction period followed by its monotonic formation. Hypochlorous acid gives the same concentration profile as the sulfinic and sulfonic acids but only at much lower concentrations.

TABLE 3: Cysteine−Chlorine Dioxide Mechanism

no.	reaction	k_f; k_r
Q1	$RCH_2SH + 2ClO_2(aq) + H_2O \rightarrow RCH_2SOH + 2HClO_2$	405
Q2	$RCH_2SOH + HClO_2 \rightarrow RCH_2SO_2H + HOCl$	5×10^3
Q3	$RCH_2SO_2H + HClO_2 \rightarrow RCH_2SO_3H + HOCl$	2.5×10^3
Q4	$RCH_2SH + HClO_2 \rightarrow RCH_2SOH + HOCl$	8×10^3
Q5	$RCH_2SH + HOCl \rightarrow RCH_2SOH + H^+ + Cl^-$	5×10^3
Q6	$RCH_2SOH + HOCl \rightarrow RCH_2SO_2H + H^+ + Cl^-$	8×10^3
Q7	$RCH_2SO_2H + HOCl \rightarrow RCH_2SO_3H + H^+ + Cl^-$	5×10^3
Q8	$RCH_2SOH + 2ClO_2(aq) + H_2O \rightarrow RCH_2SO_2H + 2HClO_2$	5×10^2
Q9	$RCH_2SO_2H + 2ClO_2(aq) + H_2O \rightarrow RCH_2SO_3H + 2HClO_2$	210
Q10	$RCH_2SH + ClO_2^- + H^+ \rightarrow RCH_2SOH + HOCl$	75
Q11	$RCH_2SOH + ClO_2^- + H^+ \rightarrow RCH_2SO_2H + HOCl$	1.2×10^2
Q12	$RCH_2SO_2H + ClO_2^- + H^+ \rightarrow RCH_2SO_3H + HOCl$	1×10^2
Q13	$2HClO_2 + HOCl \rightleftharpoons 2ClO_2(aq) + H^+ + Cl^- + H_2O$	1.01×10^6; 1×10^2
Q14	$ClO_2^- + H^+ \rightleftharpoons HClO_2$; K_a^{-1}	1×10^9; 1.02×10^7
Q15	$RCH_2SH + H^+ \rightleftharpoons [RCH_2SH_2]^+$; K_b	1×10^3; 5×10^9

TABLE 4: Mechanism Used for Modeling the Whole Reaction Scheme

no.	reaction	rate constants: k_f; k_r
S1	$ClO_2^- + H^+ \rightleftharpoons HClO_2$; K_a^{-1}	1×10^9; 1.02×10^7
S2	$RCH_2SH + H^+ \rightleftharpoons [RCH_2SH_2]^+$; K_b	1×10^3; 5×10^9
S3	$RCH_2SH + ClO_2^- + H^+ \rightarrow RCH_2SOH + HOCl$	75
S4	$RCH_2SH + HClO_2 \rightarrow RCH_2SOH + HOCl$	8×10^3
S5	$(RCH_2S)_2 + ClO_2^- + H^+ + H_2O \rightarrow 2RCH_2SOH + HOCl$	1×10^2
S6	$RCH_2SOH + ClO_2^- + H^+ \rightarrow RCH_2SO_2H + HOCl$	1.2×10^2
S7	$RCH_2SO_2H + ClO_2^- + H^+ \rightarrow RCH_2SO_3H + HOCl$	1×10^2
S8	$RCH_2SH + HOCl \rightarrow RCH_2SOH + H^+ + Cl^-$	5×10^3
S9	$RCH_2SOH + HOCl \rightarrow RCH_2SO_2H + H^+ + Cl^-$	8×10^3
S10	$RCH_2SO_2H + HOCl \rightarrow RCH_2SO_3H + H^+ + Cl^-$	5×10^2
S11	$(RCH_2S)_2 + 2ClO_2(aq) + 2H_2O \rightarrow 2RCH_2SOH + 2HClO_2$	1×10^2
S12	$RCH_2SH + 2ClO_2(aq) + H_2O \rightarrow RCH_2SOH + 2HClO_2$	5×10^2
S13	$RCH_2SOH + 2ClO_2(aq) + H_2O \rightarrow RCH_2SO_2H + 2HClO_2$	1×10^3
S14	$RCH_2SO_2H + 2ClO_2(aq) + H_2O \rightarrow RCH_2SO_3H + 2HClO_2$	210
S15	$ClO_2^- + HOCl + H^+ \rightleftharpoons Cl_2O_2 + H_2O$	1.01×10^6; 0.1
S16	$Cl_2O_2 + ClO_2^- \rightleftharpoons 2\,ClO_2(aq) + Cl^-$	1.5×10^3; 5.5×10^{-6}
S17	$RCH_2SH + Cl_2O_2 + H_2O \rightarrow RCH_2SOH + 2HOCl$	15
S18	$RCH_2SOH + Cl_2O_2 + H_2O \rightarrow RCH_2SO_2H + 2HOCl$	1×10^2
S19	$RCH_2SO_2H + Cl_2O_2 + H_2O \rightarrow RCH_2SO_3H + 2HOCl$	25

Modeling the Whole Reaction Scheme. A simplified mechanism that was distilled from the full mechanism given in Table 1 was used for modeling the overall reaction kinetics. A number of assumptions were made in arriving at this simplified scheme shown in Table 4. Reaction M2 was assumed, in this environment, to be very fast and was eliminated. Thus, it was combined with reaction M4 to give a new reaction, S3, which though termolecular, was treated as bimolecular. Reactions of chlorine dioxide were also handled in the same manner, combining M12 + M13, M14 + M15, M16 + M17, and M18 + M19 into composite reactions which were still treated as bimolecular. The kinetics constants for reactions S1 and S2 were estimated from the pK_a of chlorous acid[33] and an estimated value for pK_b of the thiol group in cysteine. The simulations were insensitive to the values of these constants as long as they were fast and not rate-determining. Thus after estimating k_{S1}, the value of k_{-S1} was then fixed by the K_a of chlorous acid. Kinetics constants for reactions S11−S14 were estimated from this study; and those for reactions S15 and S16 were derived from established literature values. The rest of the constants were adjusted for best fit. This mechanism was simulated using both the semi-implicit fourth-order Runge Kutta techniques and the Chemical Kinetics Simulator developed by IBM. The presence of rapid reactions S1 and S2 made the overall mechanism extremely stiff with calculations needing to proceed overnight on the fastest Pentium IV processors. This model was able to satisfactorily predict the data on chlorite variations shown in Figure 3 as well as that in Figure 7. It was unable to predict, to the same degree of precision, the second phase of chlorine dioxide formation shown in Figure 4. One major reason for this failure is the unknown activity of aqueous chlorine dioxide at various pHs and temperatures. The reactions we studied are known to be extremely exothermic.[35] Although we tried to control the temperature as efficiently as possible, after long periods we still lost a lot of chlorine dioxide due to its volatility.

Conclusion

The oxidation of cysteine, in the absence of P450-type enzymes and flavin-containing monooxygenases, proceeds only as far as cysteic acid. This appears to be common to all thiols with an amino group at the β or γ positions. The carboxylic acid group on cysteine, however, precludes any formation of chloramines as has been observed with taurine and hypotaurine.

Acknowledgment. We thank the University of the Western Cape for awarding a leave of absence to one of us (J.D.). We would like to thank Fungai Mukome for performing the ICPMS

analysis on the Nanopure water used for reagent preparations. This work was funded by Grant No. CHE 0137435 from the National Science Foundation.

References and Notes

(1) Kelly, M.; Lappalainen, P.; Talbo, G.; Haltia, T.; van der Oost, J.; Saraste, M. *J. Biol. Chem.* **1993**, *268*, 16781−16787.
(2) Hofgen, R.; Kreft, O.; Willmitzer, L.; Hesse, H. *Amino Acids* **2001**, *20*, 291−299.
(3) Young, V. R.; Wagner, D. A.; Burini, R.; Storch, K. J. *Am. J. Clin. Nutr.* **1991**, *54*, 377−385.
(4) Grazioli, L.; Casero, D.; Restivo, A.; Cozzi, E.; Marcucci, F. *J. Biol. Chem.* **1994**, *269*, 22304−22309.
(5) Parcell, S. *Altern. Med. Rev.* **2002**, *7*, 22−44.
(6) Stipanuk, M. H. *Annu. Rev. Nutr.* **1986**, *6*, 179−209.
(7) Halliwell, B.; Gutteridge, J. M. *Arch. Biochem. Biophys.* **1990**, *280*, 1−8.
(8) Halliwell, B.; Gutteridge, J. M. *Lancet* **1984**, *2*, 1095.
(9) Halliwell, B.; Gutteridge, J. M. *Lancet* **1984**, *1*, 1396−1397.
(10) Mirazimi, A.; Svensson, L. *J. Virol.* **1998**, *72*, 3887−3892.
(11) Carelli, S.; Ceriotti, A.; Cabibbo, A.; Fassina, G.; Ruvo, M.; Sitia, R. *Science* **1997**, *277*, 1681−1684.
(12) Chinake, C. R.; Simoyi, R. H. *Journal of Physical Chemistry* **1993**, *97*, 11569−11570.
(13) Darkwa, J.; Mundoma, C.; Simoyi, R. H. *J. Chem. Soc., Faraday Trans.* **1998**, *94*, 1971−1978.
(14) Jaenicke, R. *Naturwissenschaften* **1996**, *83*, 544−554.
(15) Han, D.; Handelman, G.; Marcocci, L.; Sen, C. K.; Roy, S.; Kobuchi, H.; Tritschler, H. J.; Flohe, L.; Packer, L. *Biofactors* **1997**, *6*, 321−338.
(16) Saez, G.; Thornalley, P. J.; Hill, H. A.; Hems, R.; Bannister, J. V. *Biochim. Biophys. Acta* **1982**, *719*, 24−31.
(17) Hogg, P. J. *Redox Rep.* **2002**, *7*, 71−77.
(18) Okazaki, R.; Goto, K. *Heteroat. Chem.* **2002**, *13*, 414−418.
(19) Makarov, S. V.; Mundoma, C.; Penn, J. H.; Svarovsky, S. A.; Simoyi, R. H. *J. Phys. Chem. A* **1998**, *102*, 6786−6792.
(20) Hirschberger, L. L.; Hou, Y. C.; Stipanuk, M. H. *FASEB J.* **1994**, *8*, A463.
(21) Thomas, E. L.; Bozeman, P. M.; Jefferson, M. M.; King, C. C. *J. Biol. Chem.* **1995**, *270*, 2906.
(22) Indelli, A. *J. Phys. Chem.* **1964**, *68*, 3027−3031.
(23) Kern, D.; Kim, C.-H. *J. Am. Chem. Soc.* **1965**, *87*, 5309−5313.
(24) Brauer, G. *Handbook of Preparative Organic Chemistry*; Academic Press: New York, 1963; p 301.
(25) Chinake, C. R.; Simoyi, R. H. *J. Phys. Chem. B* **1997**, *101*, 1207−1214.
(26) Chinake, C. R.; Simoyi, R. H. *J. Phys. Chem. B* **1998**, *102*, 10490−10497.
(27) Gordon, G. *J. Am. Water Works Assoc.* **2001**, *93*, 163.
(28) Jia, Z.; Margerum, D. W.; Francisco, J. S. *Inorg. Chem.* **2000**, *39*, 2614−2620.
(29) Chinake, C. R.; Mundoma, C.; Olojo, R.; Chigwada, T.; Simoyi, R. H. *Phys. Chem. Chem. Phys.* **2001**, *3*, 4957−4964.
(30) Huang, K. P.; Huang, F. L. *Biochem. Pharmacol.* **2002**, *64*, 1049−1056.
(31) Taube, H.; Dodgen, H. *J. Am. Chem. Soc.* **1949**, *71*, 3330−3336.
(32) Karoui, H.; Hogg, N.; Frejaville, C.; Tordo, P.; Kalyanaraman, B. *J. Biol. Chem.* **1996**, *271*, 6000−6009.
(33) Cotton, F. A.; Wilkinson, G. *Advanced Inorganic Chemistry*, 5th ed.; John Wiley; Wiley-Interscience: New York, 1988; p 567.
(34) Peintler, G; Nagypal, I; Epstein, I. R. *J. Phys. Chem.* **1990**, *94*, 2954−2960.
(35) Chinake, C. R.; Simoyi, R. H. *S. Afr. J. Chem.* **1997**, *50*, 220−226.